Received: 20 03 2025 | Revised: 10 04 2025 | Accepted: 25 04 2025

DOI: 10.15294/jim.v7i1.22583

Page 1 - 25

JIM: Jurnal Inovasi Mesin

A comprehensive study of infrastructure failures in the energy industry to improve operational safety

Dhanies Wahyu Ardyrizky[1,2], Aditya Rio Prabowo[1,*], Seung Jun Baek[3], Quang Thang Do[4]

1 Department of Mechanical Engineering, Universitas Sebelas Maret, Surakarta, Indonesia
2 Lab. Design and Computational Mechanics, Faculty of Engineering, Universitas Sebelas Maret, Surakarta, Indonesia
3 Advanced-Green Technology Center, Korea Marine Equipment Research Institute, Busan, South Korea
4 Department of Naval Architecture and Ocean Engineering, Nha Trang University, Nha Trang, Viet Nam
*aditya@ft.uns.ac.id

Keywords:
MOV
Pipline corrosion
Oil storage tank
FEA
Risk analysis

Abstract
The oil and gas industry is critical to the global energy supply. However, it is accompanied by high risks. Significant losses in terms of safety, the environment, and the economy are caused by failures in infrastructure, especially MOV, piping systems, and storage tanks. This paper thoroughly reviews infrastructure failures in the energy sector, focusing on how numerical methods can enhance safety, reliability, and efficiency. Finite element analysis (FEA), particularly computational fluid dynamics (CFD), is a key method in failure analysis. Meanwhile, reliability-availability-maintainability (RAM), failure mode and effect analysis (FMEA), and probabilistic risk assessment (PRA) are preventive methods. The study found that lubrication significantly affects MOV performance, corrosion threatens piping systems, and temperature control is vital to tank oil quality. Using numerical methods makes it possible to detect potential failures earlier, optimize maintenance schedules, improve system design, and reduce operational risks and costs in the energy industry.

1 Introduction

Energy is essential to life and technological development [1], [2]. The oil and gas industry is a key stakeholder in the global economy. It encompasses exploration, refining, processing, transportation, distribution, and sales [3], [4]. Energy is generally defined as the ability to perform work. Various activities require energy, ranging from biological development to large-scale industrial processes. As a civilization's technology advances, more energy is required to function. Currently, fossil fuels are the leading source of global energy. However, they emit high levels of pollutants [5], [6]. The oil and gas industry has become integral to other industries, including power generation, transportation, and industrial plants. As demand increases, so does the size of the energy industry. Therefore, sufficient security is necessary to ensure operational continuity and safety.

Safety is paramount in the energy sector, particularly in oil and gas and nuclear power. Most lagging safety indicators show a slight improvement in the oil and gas industry. A risk management system is needed to identify priority areas for improvement [7]. Several methodologies can identify potential failures, allowing them to eliminate or reduce the risk to an acceptable level [8].

In recent decades, numerical methods have been adopted to enhance the effectiveness and efficiency of safety analysis processes, especially in identifying risks, monitoring conditions, and optimizing hazard mitigation strategies. Numerical methods such as finite element analysis (FEA) and computational fluid dynamics (CFD) are widely used in the petroleum and gas sector due to their adaptable modeling and

This is an open access article under the terms of the Creative Commons Attribution License, which permits use, distribution and reproduction in any medium, provided the original work is properly cited.

ISSN 2746-7694

© 2025 JIM: Jurnal Inovasi Mesin.

precise results. These methods are extensively used to examine the structural integrity of critical components, such as pipes and tanks [9], [10], [11]. Other approaches incorporate failure probability modeling and risk-based maintenance analysis, such as probabilistic risk assessment (PRA) and reliability, availability, and maintainability (RAM) analyses. Data-centric and mathematical model-based numerical methods assist in the timely diagnosis of failures, enabling remedial actions to be taken. These approaches include fluid flow simulation for determining pipe strength, imperfection analysis, and design optimization, emphasizing safety and efficiency.

The oil and gas industry is increasingly using advanced technology, with control systems and automated machines for added efficiency and safety [12]. While the integration of innovative technologies offers many benefits, it also raises concerns about the interaction between humans and technology [13]. In addition to the potential risk of replacing humans, it is crucial to understand the safety of components to ensure worker safety [14]. This paper summarizes several infrastructures used in the energy industry based on safety and numbers. First is the motor-operated valve (MOV), which operates automatically and is controlled remotely. Second is the piping system, an intermediary for transferring fluids in large quantities. Third is the storage tank, which stores and maintains the oil quality until it is sold. It is a critical component that must be considered regarding strength and safety.

2 Motor-operated valve (MOV)

MOV is an electric motor with remote control technology. The main components consist of a motor, actuator, and valve. There is a pinion gear as a shaft, which is driven by a drive gear [15], [16]. In some cases, MOV controls piping flow with MOV as the main driver, especially in the oil and gas industry and nuclear power plants. The use of MOVs is generally based on high risks in the energy processing industry, predominantly nuclear. The MOV installation at the NPP aims to transfer radioactive nuclear elements to the reactor safely and accurately [17]. Limiting direct contact with humans is one of the steps to reduce the risk of accidents. One of the critical parameters related to the aging effect of the actuator is the stem factor. Which is defined as the ratio of the stem torque to the stem thrust. The stem factor only depends on the stem friction coefficient if the manufacturer knows the geometry of the stem and the stem nut [18].

The actuator case is operated by a motor, where the motor provides the main power. The lubrication system is related to the stem factor, the friction coefficient of the stem, and the stem nut. Differential equations control the movement of the stem and the stem nut. Lubricants were determined using the same injection method without reference to testing intervals. The lubricant types are Albania P2, Unirex N2, Mobil EP0, Texaco EP2, and Multifak EP2. Additional considerations were obtained through calculations of physical parameters, such as pitch diameter, the gap between the stem and stem nut, speed, acceleration, force, and friction coefficient, as shown in Table 1 [18]. The ROL phenomenon can cause a significant loss of thrust when its value increases with increasing pressure difference. The pressure difference significantly affects the stem factor and the thrust magnitude, but does not affect the torque much [16]. In the paper [15], four relationships are explained and modeled with a differential form presented in Equation (1) describing the system's dynamics. While the analysis was focused on a blended oil with 75 cP dynamic viscosity, variations for 150 cP and 300 cP viscosities were also considered. It was concluded that the equilibrium equation of the thrust force cannot be solved without solid contact. Experiments were conducted under dynamic conditions with defined boundaries using lubricants containing various mixtures of 50.85% kerosene and base oil. The properties of these lubricants are shown in Table 2.

Table 1. Design and operational information for tested valves.

Valve manufacturer	Actuator manufacturer	Stem pitch (in)	Stem lead (in/rev)	Lubricant	Actuator operating years	Operational temperature (°F)
Samshin	Nippon Gear	0.17–0.4	0.17–0.8	Mobile 28, Mobile EP0, Multipack	Less than 10 years	More than 60 ◦F

				EP0, Texaco EP2	
Westinghouse	Limitorque	0.2–0.33	0.225–0.67	Alvania EP2, Mobile EP0, Txaco EP2	More than 18 years
Velan	Limitorque	0.167–0.5	0.2–1.0	Alvania EP2, Mobile EP0, Multipack EP0	More than 6 years
	Jocomatic	0.2–0.33	0.25–0.75	Unirex N2	16–17 years

Table 2. The property of kerosene at the initial condition

Name		Remaks
ρ_{Kero0}	800 kg/m³	Density
$\mathcal{V}_{Kero0}$	2.39 cSt	Kinematic Viscosity
μ_{Kero0}	1.912 cP	Dynamic Viscosity
α_{Kero}	0.119 GPa^{-1}	Pressure viscosity coefficient
β_{Kero0}	1.39 Gpa	Bulk modulus
β_{Kero1}	0.270	Ratio of bulk modulus change to pressure change

A coefficient of friction increases from 0.095 at 0.919s to 0.141 at 0.422s before the seating point, with 94% of the normal force contributed by solid contact. After the seating point, the friction coefficient becomes 0.105 at 4.587s, which changes the solid contact force to 70%. By reducing the normal force after the sitting position, the shear force decreases due to the correlation of the friction coefficient, which is the division of the shear force by the normal force. With these results, it can be concluded that the numerical solution of the differential equation can be helpful in design calculations such as thread surface distance, velocity, and acceleration related to the friction coefficient.

2.1 Friction factor

Table 3. Subjects related to MOV's friction behavior

No.	Scholars	Subjects	Findings
1	Kim et al. [15]	Transient analysis of lubrication with a squeeze film effect due to the loading rate at the interface of a motor-operated valve assembly in nuclear power plants	Changes in the stem's coefficient of friction were caused by the change of shear force in solid contact mode during the switching process between solid and fluid contact modes.
2	Kang et al. [18]	Stem friction coefficient behavior of motor-operated valves	Most coefficients change randomly, neither increasing nor decreasing continuously over time. Under certain conditions, higher coefficient values may be observed, but these values are susceptible to decrease.
3	Kim et al. [17]	Effect of lubrication performance on motor-operated valve actuator output thrust	The SFC value of the old lubricant appears to be higher than the new lubricant, and the old lubricant at the TST point produces a lower thrust value than the new lubricant at the same torque value. SFC is an instrumental variable in analyzing lubrication performance quantitatively.

4	Kim et al. [16]	Study on the phenomenon of rate of loading in motor-operated gate valves	The ROL appears to become higher as the differential pressure increases, and in high differential pressure conditions, it accounts for about 17.6% of the thrust loss. In addition, the ROL effect is negligible in valves with low differential pressure (below 1100 kPa).

The friction coefficient depends on the stem lead and the pitch diameter. The effect of the loading rate also influences the thread friction coefficient, which changes between the static stroke (high loading speed) and the dynamic stroke (low loading speed). The study in [18] is based on data obtained from static conditions. The data was obtained from diagnostic testing of 20 MOVs on Korean nuclear power plants in 1999.

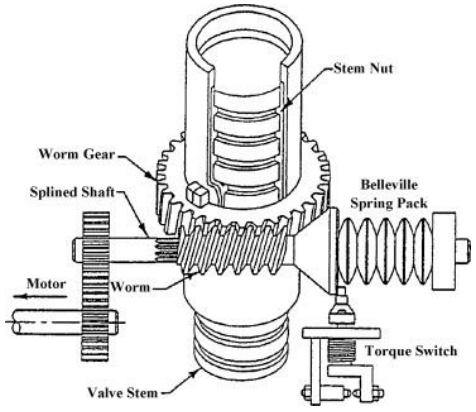

Figure 1. MOV actuator components: stem nut and stem [16].

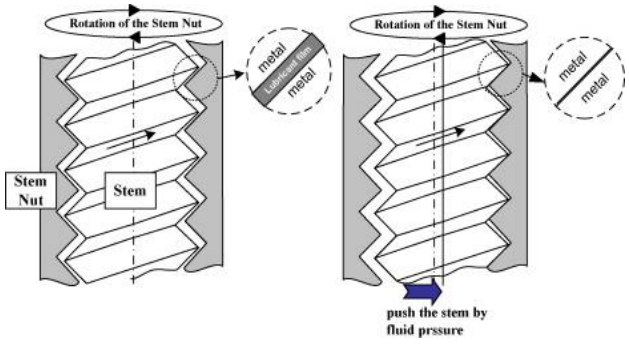

Figure 2. Friction between the stem nut and the stem. [16].

Testing was carried out at least twice for each valve, namely basic design tests and periodic tests. The calculation of the friction coefficient uses torque and thrust data measured on the strain gate sensor installed on the stem. The equation used

$$\mu = \frac{0.96815 \cdot 24 \cdot SF - (l_0/\pi)}{24 \cdot SF \cdot (l_0/\pi \cdot d_{pitch}) + d_{pitch}} \quad (1)$$

After processing and compiling graphs from the data [18], the analysis found no degradation pattern for the three types of MOV manufacturers. It reviewed geometry, lubricant type, MOV life, and operating temperature, and compiled graphs. It can be concluded that the geometry of the stem does not affect the degradation potential.

2.2 Risk Evaluation

Pioneer research [8] has developed an innovative AI-augmented tool. It is called "AI-FMEA." The tool performs Design Failure Mode and Effects Analysis (d-FMEA) and Failure Mode, Effects, and Criticality Analysis (d-FMECA). This method integrates AI, specifically artificial neural networks, into the traditional D-FMEA/FMECA process. The primary objective of this method is to transform a complex process into an easy-to-use, AI-enhanced process. The tool features a user-friendly graphical user interface (GUI) and a statistical backend system. This system uses Weibull, Rayleigh, and Bathtub distribution-based methods to analyze and predict failure rates over time.

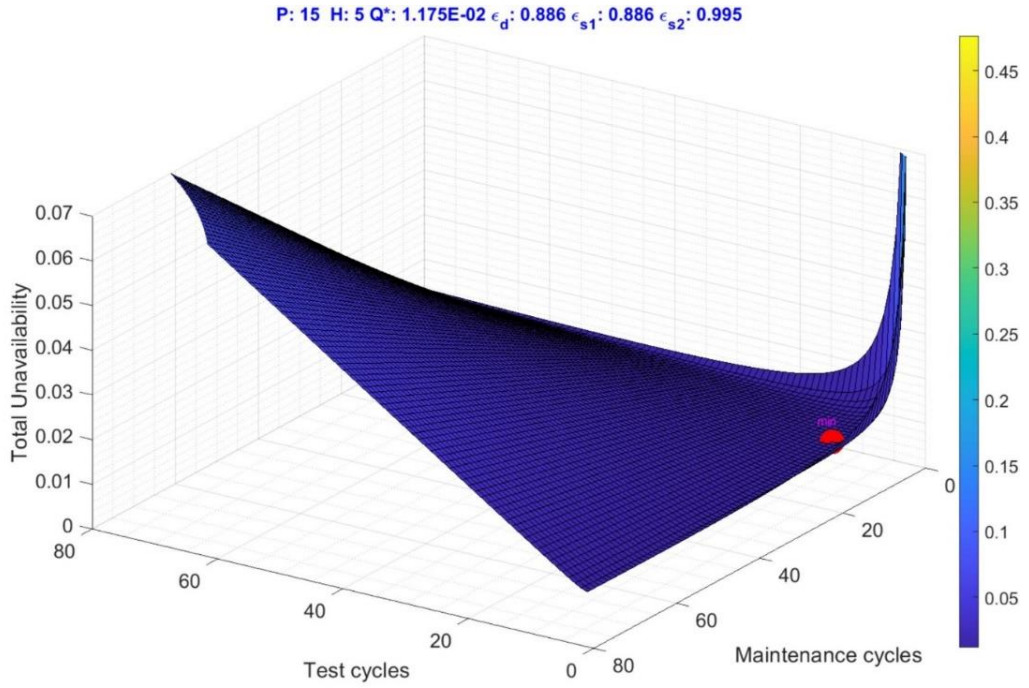

Figure 3. Diagram of unavailability relationships with different maintenance scenarios [19].

Reliability, availability, and maintainability (RAM) is a model of the relationship between safety and components, explicitly with the correlation of aging effects, maintenance effectiveness, operational conditions, test efficiency, and imperfect aging and testing factors causing degradation due to stress that occurs [19], [20]. RAM is a function of inherent component reliability, with the level of component failure caused by design, aging, degradation, and the effectiveness of testing and maintenance. Imperfect maintenance affects the age of goods and their performance. Imperfect maintenance can affect service life to a certain extent. In addition, in the literature of [21], aging factors can affect mechanical and electrical failures in MOVs. MOVs with electric actuators are more susceptible to aging, primarily if they operate in high-radiation environments. The method involves formulating an optimization problem to determine the optimal number of surveillance tests (STs) and preventive maintenance (PM) activities during a specified refurbishment period [19], [20]. As a case study, it was applied to Motor-Operated Valves (MOVs) in a High-Pressure Injection System (HPIS) at a VVER/1000-V446 nuclear power plant. Each HPIS unit remains in standby mode during regular operation to maintain a coolant supply to the reactor core. The optimization problem was solved for a 10-year (87,600-hour) refurbishment period. The discussion highlights that increasing monitoring tests can reduce the number of preventive maintenance activities required to minimize unavailability. It also notes that a combination of five monitoring tests and fifteen maintenance tasks results in the lowest unavailability in specific scenarios. Figure 3 shows the relationship between the number of test cycles, maintenance cycles, and unavailability. However, increased testing and maintenance can lead to component degradation [19], [20].

Table 4. Related study to evaluate the risk of MOV

No.	Scholars	**Subjects**	**Findings**
1	Li et al. [22]	Risk evaluation for motor-operated valves in an in-service testing Program at a PWR nuclear power plant in Taiwan	IST Risk-Based Evaluation can benefit industrial personnel by identifying system vulnerabilities, reducing unnecessary testing burden, concentrating testing resources on critical path-oriented valves, and reducing dose exposure.
2	Parsaei et al. [19]	Risk-effective optimal maintenance regime for a periodically tested safety	The most rational optimal ST&M should be determined as simultaneously aligning and positioning within a wide

		component subjected to imperfect repair	margin of risk effectiveness while also meeting the criteria outlined in the RMTS framework.
3	Grabill et al. [8]	AI-augmented failure modes, effects, and criticality analysis (AI-FMECA) for industrial applications	The new AI-driven tool offers significant time and effort savings when performing d-FMECA, a labor-intensive engineering task. In addition, the tool can be used to train professionals in risk and reliability.
4	Parsaei et al. [20]	Effect of test-caused degradation on the unavailability of standby safety components	Research shows that other models do not simultaneously consider the full effects of degradation and maintenance impacts. The proposed model can more realistically evaluate the availability of safety components and related systems.
5	Martón et al. [21]	Optimization of test and maintenance of aging components consisting of multiple items, and addressing effectiveness	The optimization algorithm provides the best solution for formulating and solving the optimization problem, considering complete flexibility in implementing testing and maintenance activities in an integrated RAM model.
6	Shin et al. [23]	Surveillance test and monitoring strategy for the availability improvement of standby equipment using an age-dependent model	Compared with traditional deterministic PSA approaches, the proposed method can provide more realistic and detailed unavailability information over time. It can thus be applied to dynamic PSA or risk-considered regulations.
7	Ting et al. [24]	Risk-informed developments and comparisons for the safety-related valves of the Inservice Testing Program at Taiwan BWR and PWR nuclear power plants	Applying the RI-IST (Risk-Informed Inservice Testing) approach to MOV allows for reduced testing frequency. For example, for MOV in PWR, the testing frequency can be reduced from 5460 times to 3786 times in 10 years, thus reducing personnel dose exposure and outage costs without compromising safety.
8	Song et al. [25]	Comparison of state-of-the-art correlation effect associated with lognormal, beta, and gamma uncertainty distributions	The effect of SOKC on MOV is more significant if the uncertainty is modeled with a lognormal distribution than a gamma or beta distribution when the parameters of both distributions are estimated based on the same failure data using the method of moments.
9	Kim et al. [26]	Rigorous derivation of interfacing system LOCA frequency formulas for probabilistic safety assessment of nuclear power plants	A case study was conducted on Optimal Power Reactor 1000 (OPR-1000), where MOVs were analyzed as part of the ISLOCA potential path. The new method's ISLOCA frequency calculation was more accurate than the old method's, especially under conditions where MOVs have the same failure rate.
10	Kordalivand et al. [27]	Quantifying the impact of risk mitigation measures using SPAR-H and RCM Approaches: Case study based on VVER-1000 systems	The implementation of the RCM strategy in this study shows that the probability of MOV failure can be reduced by up to 5%. Improved operator training can also reduce the possibility of human error impacting MOV operations.

Considering uncertainty in probabilistic models, State of Knowledge Correlation (SOKC) helps improve the accuracy of equipment failure estimates, including MOV. The impact of SOKC on failure analysis with lognormal and gamma distributions is assessed using the probabilistic risk assessment (PRA) method. The influence of SOKC is more significant on lognormal distributions, especially when the number of correlated components increases. This impacts Reliability, Availability, and Maintainability (RAM), where aging effects, maintenance effectiveness, and test imperfections can cause MOV to deteriorate over time due to correlation. Figure 3 shows the relationship between the number of testing and maintenance cycles and unavailability values. More testing and maintenance can cause component degradation.

To identify components with a high level of safety (High Safety Significant Components, HSSCs), risk evaluation is carried out based on Probabilistic Risk Assessment (PRA) on valves operated by MOV. The IST program is prepared based on ASME Boiler & Pressure Vessel Code section XI to ensure the valve

continues to operate correctly. PRA can identify valves that have a high impact on safety, such as MOV, so that it can be focused on the most critical components [24]. The benefits of IST can save costs from maintenance, reduce the number of workers or officers when testing, and reduce radiation exposure for staff [22], [24]. Evaluation of Structure, System, and Component (SSC) can be identified in numerical results, and testing or observation can be combined on High Safety Significant Components (HSSCs) with a plan to maintain the company's philosophy regarding safety and cost. In paper [22], RI-IST is also applied, focusing on safety-related valves on 146 MOV.

Unavailability models generally consider two types of stress that cause component degradation. Standby stress is related to the time and age of the component. Demand stress occurs when the component works in a dense cycle [20]. In the paper, the availability model that depends on the aging age comprehensively for standby equipment that operates according to actual time. Two strategies to improve equipment availability have been developed from the model. The first is the Online Monitoring-based Inspection Method (OMIM), which observes elements over time without actual operation. Second, the Shortening Surveillance Test Interval Method (SSTIM) adjusts the testing interval based on the age of the equipment. In actual calculations, MOV is an example of standby equipment. Testing every 2200 hours (estimated 92 days) yields a q_{ave} of 0.0404. For minimum results, when testing every 40 days, q_{ave} 0.0323. When testing for 10 days, q_{ave} 0.0615. For the second case scenario, when the move is in the initial installation state, periodic testing is carried out at 40-day intervals, and failure is considered 15 years after testing. The overall average equipment unavailability is more significant in case 2 than in case 1 because the aging effect is stronger than the effect of replacing certain elements. In this case, the optimal test interval is 15 days, and q_ave is 0.0424. OMIM assesses the condition of some elements without actual operation through short sensing intervals sensitive to standby time, reducing component availability. Additionally, OMIM shows that with 100% coverage, the optimal testing interval can be extended to 360 days. SSTIM can complement OMIM by adjusting the surveillance test interval based on the component age. SSTIM can even reduce unavailability by up to 82% compared to a fixed test interval. Both methods provide the best test plan and recommendations for more effective maintenance activities regarding standby time [23].

3 Piping

Terminals are essential to the oil's temporary storage and transportation system. Still, leaks threaten the environment and safety and can be caused by corrosion, weakened pipe strength, and abrasive materials [28]. Piping systems are a critical component in distributing energy and fuel supplies. The piping system helps flow fluids from one place to another efficiently and effectively. The transportation of emulsions (oil%-water%-gas%) is challenging for oil companies because complex chemical reactions occur, considering the different piping geometry and flow patterns [29]. The strength of the piping is an important aspect that needs to be considered for operational safety. The selection of pipe materials is difficult for designers because they must consider several things, such as strength, weight, environmental conditions, fluid type, and cost. Where the suitability of needs and budget must be in line, several standards and regulations must be met to ensure the safety and operation of components. The main challenges in piping design are energy efficiency and the factors that cause pipe failure. Corrosion, pressure, vibration, and temperature fluctuations can affect the durability of piping systems, causing failure or operational disruption. Carbon steel is commonly used as the primary material for piping systems because of its cheapness and high availability despite its low corrosion resistance. Carbon steel can form an iron oxide layer, but the ingress of acid in the oil content can cause or accelerate the corrosion rate on the protected surface [30], [31]. Careful and accurate design, manufacturing, and maintenance can solve these problems. This will increase productivity and reduce the risk of accidents and financial losses. Therefore, the application of FEM allows for efficient and effective mitigation of complex cases [32].

3.1 Piping Failure

Significant pressure drops and high mass flow rates caused by various pressure-reducing devices (valves, restricted orifices, etc.) generate acoustic energy that can cause excessive vibrations in pipes and

result in dynamic stresses that pose a risk of pipe failure. Predicting the distribution of dynamic stresses in pipes under AIV using FEA is an effective method. Predicting the dynamic stress distribution in pipes under AIV using finite element analysis is adequate [32]. Study in [32] uses FEA with the assistance of ACTRAN FFT software. Numerical calculations were performed by considering the fluid during AIV as gas (light fluid). Figure 4 shows that the mesh size was selected as 15 mm. This size's magnitude enables precise wave propagation calculations, extending up to 3,000 hertz (surpassing eight wavelengths per element at this frequency). Given the high frequency of AIV, the pressure field was computed between 150 Hz and 3,000 Hz. The method was validated by measuring the components, namely, pipe failure caused by AIV. Based on field conditions, the conditions reviewed encompass the entire pipe around the crack area. The numerical computation results correlate well with the theory, stating that only plane acoustic waves exist before the threshold frequency. After the threshold frequency, transverse acoustic waves dominate. The modeling and numerical approach provides a good solution for comparing real measurements with modeling results, which can be very close depending on the initial data or boundary conditions set [30].

Evaluation of pipe fragility [30] against seismic events modeled by a numerical approach using ABAQUS software. Nonlinear dynamic analysis with 157 earthquake records. Earthquake records have PGA values ranging from 0.1g to 0.6g and PGV between 10 cm/s and 60 cm/s. This paper observes that 250000 barrels of crude oil per day is Iran's fourth-largest oil producer after Abadan. The piping system is modeled in solid and beam types; beam elements are used on straight parts to reduce computing time. The use of beam elements shows entirely accurate results with an error of 10% compared to solid elements.

Determination of the piping system mesh shown in Figure 5 is 2 cm and 5 cm for some simpler parts. There is another model, namely modeling a piping system with frame elements, that aims to reduce computing time. The records are categorized into 30 groups based on PGA and PGV values. Loading includes gravity, pressure, environmental conditions, and seismic loading. Elbow failure is usually characterized by the appearance of small holes in the elbow, which is caused by local corrosion. Methods for detecting corrosion include visual inspection, chemical/microstructural analysis, and analysis of corrosion products by observation using X-rays [31]. At the elbow, there is a maximum stress, which indicates that it is the most critical point in the piping system. If the two fragility functions are compared, the double fragility function will be superior to the single. The double fragility function provides a more accurate estimate by simultaneously considering both variables (PGA and PGV). Applying the double fragility function will be easy because PGA and PGV micro zonation maps are available in many seismic areas. Damage estimation with high accuracy can help make decisions to reduce seismic risks and impacts [30].

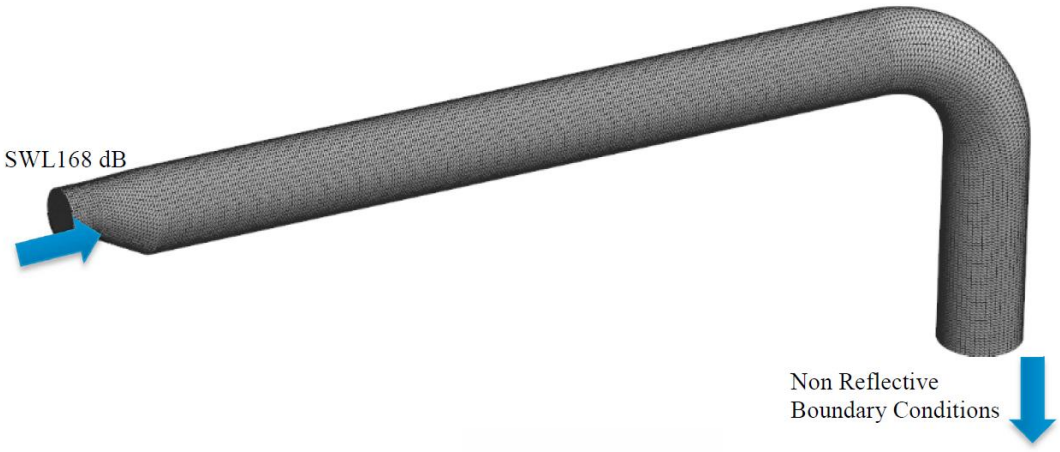

Figure 4. Acoustic finite element model

Table 5. Subjects related to the failure of piping.

No.	Scholars	Subjects	Findings
1	Hosseini et al. [30]	Development of double-variable seismic fragility functions for oil refinery piping systems	Using PGA and PGV together, as IM in developing fragility functions, provides more reliable vulnerability estimates.
2	Tawancy et al. [31]	Analysis of corroded elbow section of carbon steel piping system of an oil–gas separator vessel	A pinhole was observed to be formed due to local corrosion involving sequential chlorination and sulfidation reactions, which correlated with the formation of hydrochloric acid through the hydrolysis of inorganic salts in crude oil.
3	Coulon et al. [32]	Numerical fatigue methodology for piping systems: qualifying Acoustic Induced Vibration in the Oil & Gas industry	The methodology allows us to assess the direct impact of Acoustic Induced Vibration (AIV) mitigation measures. By applying some of the most common solutions to overcome AIV risks, a quantitative analysis has been carried out, which shows the reduction in the Likelihood of Failure (LOF) of each solution
4	Hu, Jinlong [33]	Prediction of the internal corrosion rate for oil and gas pipelines and influence factor analysis with interpretable ensemble learning	This interpretable ensemble machine learning approach outperforms other models in accuracy and interpretability, providing valuable insights for decision-making in pipeline management.
5	Madjid Meriem-Benziane et al. [34]	The effect of crude oil on pipeline corrosion caused by the naphthenic acid and the sulfur: A numerical approach	The simulation shows solid deposition (FeS and $FeCH_3COO$) develops along the pipe. Corrosion develops rapidly in the defective pipe. Changing operating conditions (pressure, temperature, and oil quality) in a CFD helps reduce the impact of corrosion.
6	Madjid Meriem-Benziane et al. [29]	Numerical study of elbow corrosion in the presence of sodium chloride, calcium chloride, naphthenic acids, and sulfur in crude oil	Numerical results prove that the corrosion location is focused on specific areas, especially at the outlet of the extrados elbow wall. Numerical results provide more solutions to avoid corrosion and improve refinery operational safety.
7	Ge et al. [35]	Numerical simulation of tubular heating in waxy crude oil vault tank based on VOF model	Quick estimation of the spread range of a tank leak allows identification of the location and size of the leak point.
8	Chen et al. [36]	Stress prediction of heated crude oil pipeline in permafrost region via fully coupled heat-moisture-stress numerical simulation and SVM algorithm	The leading indicators helpful in improving the pipe's ability to absorb loads and resist deformation have been obtained. In the study, the maximum axial stress of the buried pipe will not exceed 400 MPa, which is still lower than the yield strength of the pipe steel. Thus, the pipe can operate safely over a 10-year service life.

The purpose of FEM is to predict the vibration level along the pipe wall and produce accurate measurements. Pipes, supports, and flanges are modeled as shell elements. The damping ratio is assumed to be ζ=1 in modeling. Numerical modeling and approximation, or FEM, introduces a good solution to compare actual measurements with modeling whose results can be very close depending on the initial data or boundaries set [30]. Corrosion is a significant threat to the safety and reliability of oil and gas pipelines [28], [29], [31], [33], [34], [37], [38]. part from affecting the strength and durability of pipes, corrosion can also contaminate the products being distributed [33]. System pressure, fluid characteristics, and inhibitor effectiveness influence internal corrosion [29], [33]. Corrosion can be caused by HCl, H_2S, NaCl, $CaCl_2$ [33], naphthenic acid, and sulfur (S) [35] compounds contained in crude oil. Corrosion in crude oil distribution pipelines due to naphthenic acid and sulfur (S) forms small cracks and defects in the pipe walls. With the increasing need and demand for petroleum, crude oil is often transported in the form of water-in-oil emulsions to reduce viscosity [34].

However, high temperatures during transportation can trigger chemical reactions that cause or accelerate the corrosion rate. Meanwhile, in research [29], a CFD package for the study was carried out using Fluent with laminar flow conditions and an incompressible liquid with the Herschel-Bulkley flow model. Boundary conditions were determined by considering boundary conditions such as inlet velocity and outlet pressure. Initial conditions were L = 8 m, radius r = 0.205 m, velocity U: $U_r = 0$ and $U_z = U_{oil} = 0.6\ m/s$. Table 6 shows the dependencies of the rheological parameters n, K, and τ_c on the boundary. Severe corrosion occurs in some regions of the pipe, especially the outlet section. AI algorithms easily explore the relationship between corrosion-related properties, such as corrosion rate and maximum pitting depth. Even though this method seems easy to apply, many assumptions are too simplified, causing the accuracy of this method to be very poor, and collecting corrosion data from undersea oil and gas pipelines in China. Before data processing, normalization is carried out to increase the accuracy and stability of the model. With a length of 5.5 km, the influencing factors are temperature, pressure, flow rate, and pH. An ensemble learning model is trained to map the relationship between input parameters and internal corrosion rate. SHAP and ALE each function to interpret model predictions and explain the local effects of existing features. The extra tree regression (ETR) model performs best with an R^2 of 0.933 and RMSE of 0.043. Six ensemble machine learning models were used to predict the corrosion rate of deep pipes with original data, and are still valid [33].

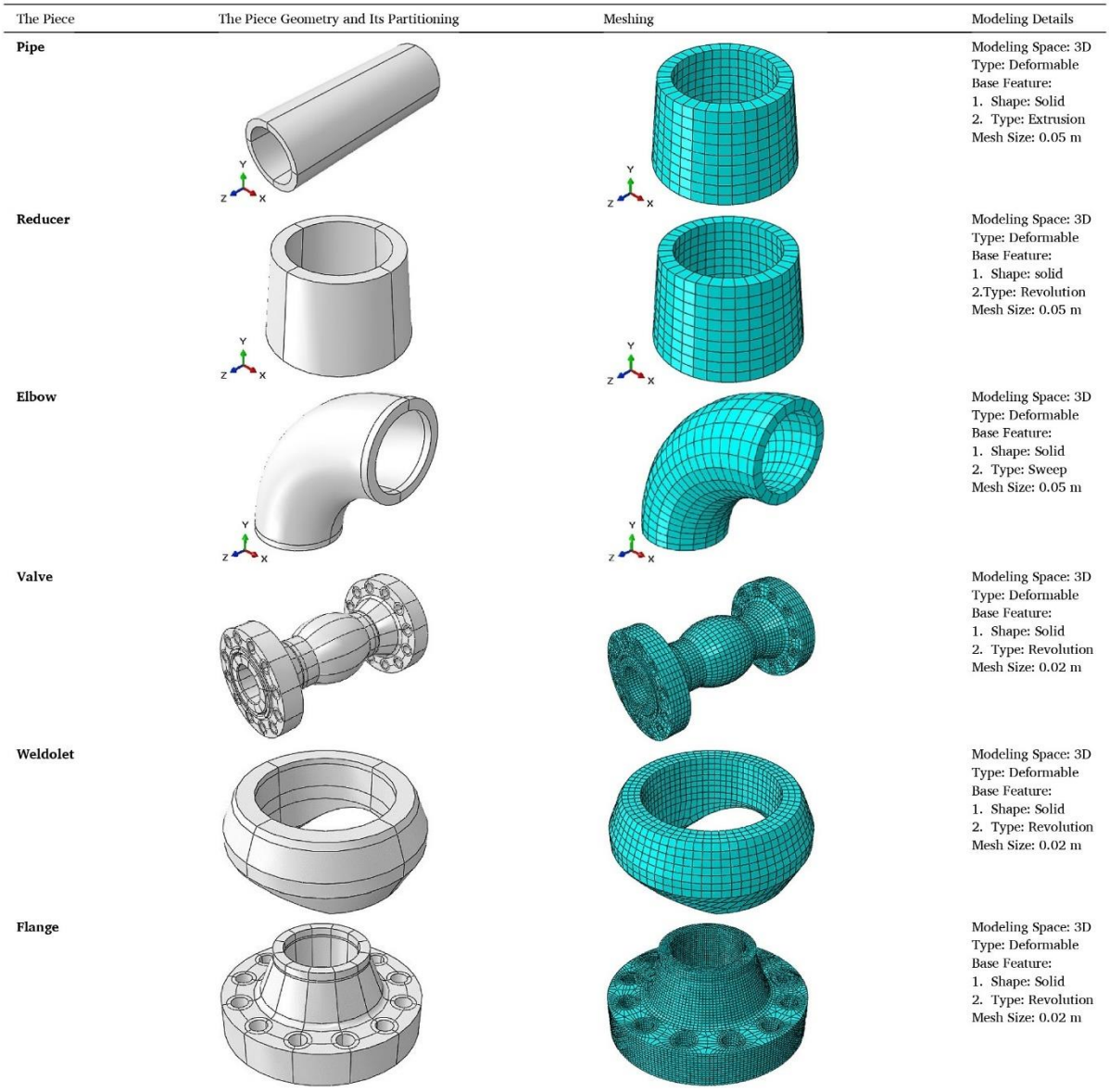

Figure 5. The pieces of the considered piping system along with their features and modeling details [30].

CFD was used for crude oil flow modeled as a non-Newtonian fluid with the Bingham model. The model also considers chemical reactions during refining, including the formation of $FeCl_2$, FeS, dan $Fe(CH_3COO)_2$ Based on the simulation results, corrosion occurred in two areas, namely, the extrados side elbow outlet and the intrados elbow arch. It was shown that the velocity increased and was maximum on the wall of the extrados elbow, causing shear stress and friction factors to affect corrosion. Research in [29] concluded that the most severe corrosion occurred at the outlet elbow on the extrados side, caused by chemical reactions between several compounds in crude oil. Pipelines that operate throughout the year cause positive temperature increases, resulting in the thawing of the surrounding soil, especially unstable permafrost in China. This thawing of the soil lowers and increases the load on the pipe, thus increasing the axial stress that occurs in the pipe. The risk of weld failure will increase, especially if there are defects in the weld joint. Manual calculation methods have not been able to predict additional axial stress induced by permafrost thawing.

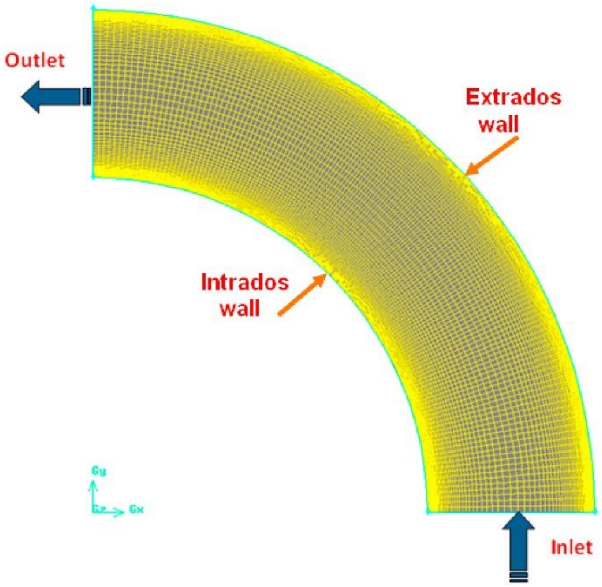

Figure 6. Mesh of elbow for two dimensions with the boundary conditions [29].

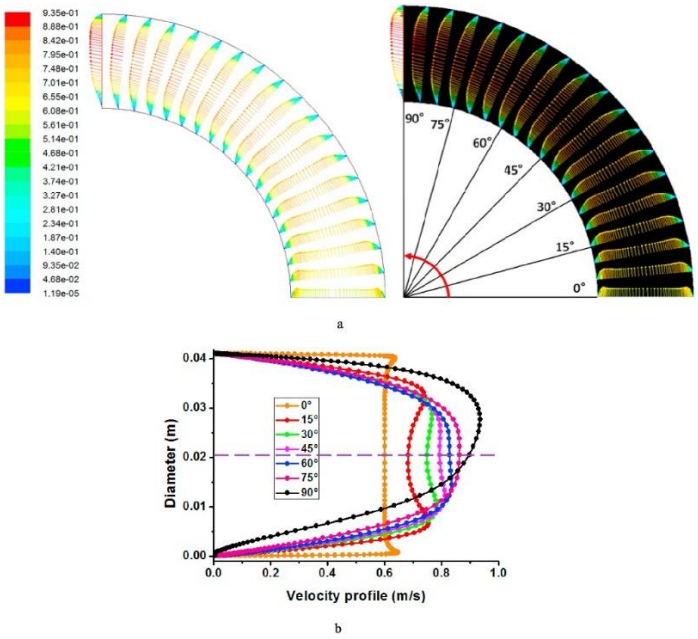

Figure 7. (a) Angle-dependent velocity vector distribution (0°, 15°, 30°, 45°, 60°, 75° and 90°) of the elbow for the Bingham model. (b) A variety of angles are shown in the velocity profile (0°, 15°, 30°, 45°, 60°, 75° and 90°) of the elbow for the Bingham model [29].

Table 6. Kerosene parameters in the Herschel-Buckley model [29].

Sample	Herschel-Buckley Model		
	τ_0 [Pa]	$K[Pa.s^n]$	n
Crude oil	0.85	0.076	0.86

Using the theory of heat conduction and permafrost melt consolidation, a numerical approach solution, an axial stress prediction model was developed with the SVR algorithm and validated with field data. Factors such as pipe thickness, insulation layer thickness, burial depth, and liquefaction zone length are the boundary conditions needed to solve this problem. The effect of pipe wall thickness will reduce axial stress and increase pipe stiffness. Pipes with insulated layers show lower axial stress than those without insulation. The burial depth will affect the amount of thawed soil, which will cause additional axial stress. The length of the thawing zone produces axial stress that varies non-linearly along the zone, with the maximum value occurring at the thawing boundary zone. The modeling has a relative error of 10% from the actual conditions in the field. Therefore, the model is accurate and can support the structural design of pipes in the liquefaction zone [36].

3.2 Oil Flow

Several methods deal with pipeline flows related to transportation issues. Unconventional oil fields are widely dispersed, making it challenging to exploit crude oil due to various issues. Estimates suggest that heavy crude oil reserves are twice the size of light crude oil reserves. Transporting heavy crude oil is challenging because it stops flowing below the pour point. High pour point, viscosity, and elasticity are heavy, wax-containing crude oil characteristics. Usually divided into three: viscosity reduction, drag/friction reduction, and crude oil conditioning [37]. The background of the difficulty of flowing crude oil in the pipeline, due to the large density and high viscosity, of course, the flow will not be efficient if it is directly flowed [39]. The principle of the dilution method is to add another oil with a lower viscosity to reduce the viscosity. Still, it requires a large volume of solvent and risks causing asphaltene deposition. The emulsification method adds water and surfactants to form an emulsion, which reduces viscosity but carries the risk of corrosion in the pipe. Friction reduction methods use additives to reduce pipe wall friction, but are less effective for heavy and high-viscosity oils. Annular and core techniques use a thin layer of water to reduce friction. The heating method is heating the oil to reduce viscosity and prevent wax formation. The ultrasonic method uses ultrasonic waves to break down hydrocarbon molecules and reduce viscosity. The microwave method breaks asphaltene particles with microwave radiation. Solar heating requires considerable capital and a long payback time. In the electromagnetic field method, the principle of the Lorentz force causes particles to move, and viscosity decreases. Thermochemical, with the same principle of heating oil but with an exothermic reaction heat source of several chemicals. Plasma heating requires high costs and in-depth risk analysis. A combination of several methods can be more effective for flowing crude oil. Electric and ultrasonic heating methods are considered more efficient and have lower operational cost [37].

Table 7. Subjects related to waxy crude oil flow.

No.	Scholars	Subjects	Findings
1	Ratnakar et al. [37]	Flow assurance methods for transporting heavy and waxy crude oils via pipelines without chemical additive intervention	Applying two or more viscosity reduction techniques of crude oil is recommended to ensure smooth flow.
2	Zhang et al. [39]	Three-dimensional numerical simulation of heat transfer and	The slope of the pipe greatly influences the natural convection caused by gravity; the temperature

		flow of waxy crude oil in inclined pipe	gradually decreases along the pipe's downward slope.
3	Madjid Meriem-Benziane et al. [34]	main influencing factors of waste heat utilization effectiveness in the tank storage Receiving process of waxy crude oil under dynamic liquid level conditions	Waste heat utilization in the crude oil receiving process is influenced by factors such as liquid level dynamics, mixing conditions, and the external thermal environment.

The density, viscosity, and heat capacity of crude oil greatly influence heat transfer [40]. Crude oil tends to be waxy when the temperature decreases, which causes pipeline blockages [37], [39]. Therefore, the cooling and wax formation processes must be analyzed to prevent pipe failure. The CFD method was used for a 3D simulation model to study the heat transfer characteristics and flow of waxy crude oil in pipes at various inclination angles (0°, 25°, and 45°). The model was created using the specifications of a segment of an overhead pipeline. This pipeline had a specific internal diameter of 219 millimeters, a wall thickness of 5 millimeters, an insulation layer of 40 millimeters, and a length of 130 meters. The pipeline is exposed to an atmospheric environment with a constant temperature of -20°C. Solid mediums (the pipe and insulation) are assumed to have isotropic physical characteristics. The initial velocity field is set to zero at the start of the shutdown simulation. The initial temperature field for the shutdown simulation is taken from stable pipeline operating conditions. The temperature distribution after the simulation shows that it occurs in three stages. A layered distribution occurs when, in the initial conditions, the temperature of the top of the pipe is higher than the bottom. Elliptical distribution: after some time, the oil cools and changes from liquid to solid. Concentric distribution occurs at the final stage, where the pipe temperature becomes uniform. The angle of inclination of the pipe affects the temperature distribution in the pipe flow. At a slope of 45°, it can be seen that the highest and lowest points of the pipe have a significant temperature difference, reaching 5,012°C. Then, the oil liquid fraction volume increased by 1,6 % [39]. In addition, a larger slope angle indicates a faster flow in the middle and upper parts of the pipe, while the flow below slows down more quickly. According to the paper [39]Gel formation with a greater slope level tends to gelate more quickly, and the lower part of the pipe is susceptible to blockage.

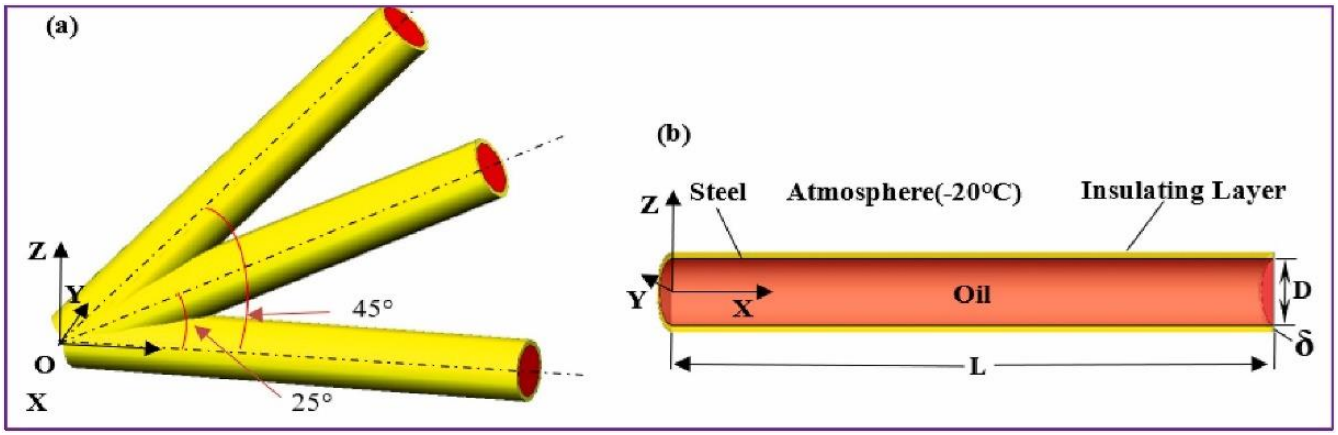

Figure 8. (a) Different inclinations of the pipeline. (b) The symmetrical structure of the pipeline [39].

4 Oil storage tanks

Various types of storage tanks can be applied according to the needs of the stored product. Vault tanks are often used for temporary storage of small quantities, while floating roof tanks are commonly used for long-term storage [41]. Facilities in the oil and gas industry that function as temporary storage places for various oils before they are distributed for processing or marketing. Storage tanks are essential in the exploration, production, and processing distribution processes. The products include crude oil, processed products, or other fuels. Based on the products stored, the shape of the storage tank can vary from cylindrical and elliptical to spherical, with a capacity that depends on needs. The selection of tank materials is generally

based on the criteria of being corrosion and pressure-resistant and equipped with a safety system to prevent leaks, fire, lightning strikes, or other environmental damage. The supporting system usually has volume, temperature, pressure measuring equipment, and remote monitoring technology. The use of storage tanks is crucial in maintaining supply availability and price stability in the market.

4.1 Temperature control

Serious problems may arise during the pouring process if crude oil is stored for a long period of time. If the accumulation and storage of crude oil is carried out for an extended period, it can cause serious problems during the pouring process. High viscosity can hinder the movement of the floating roof, on the other hand, with high viscosity, the oil can clot, resulting in reduced pump suction capacity [42]. Conventional tank heating is considered inefficient and produces high emissions [43]. Coil heating methods are currently popular, but they are not energy efficient. Coil structures can enhance natural convection and accelerate the heating process, especially under the tank. One type is the circumferential coil. However, this type has the drawback of decreased heating in the middle and upper sections of the tank. The greatest heat loss occurs at the boundaries of the tank. Thermal insulation enables oil to retain heat longer and reduce energy consumption for heating [40]. Achieving the desired quality of oil storage and distribution in cold regions requires adequate temperature control. Uneven temperature distribution can cause the oil to freeze or form wax, which can potentially lead to accidents. One proposed solution is mechanical agitation to maintain uniform temperature distribution within the tank. A limited volume method and a standard turbulence model examined crude oil transfer in a tank with a moving roof. The volume method is used for computational domain discretization with a refined grid in intense heat transfer and flow areas. The computational domain is divided based on oil heating rates into significant, indirect, and minimal influence zones in Figure 12 [35], [42]. The results show hot jet nozzles can significantly increase heating rates and mixing. The setups feature tanks of specific dimensions (e.g., 1 m in diameter and 40 cm in height). The experimentally tested variables include nozzle outlet temperatures of 48, 57, and 65 °C; nozzle diameters of 4 and 8 mm; nozzle angles of 30 and 45 degrees; and triple and quadruple nozzle arrangements. Temperature sensors are placed at different heights. The temperature difference between the nozzle outlet and the oil should be minimal to avoid stratification. Precise control of the flow velocity and temperature from the nozzle can improve efficiency by 50–70% [44]. Paper [45] used the continuity, momentum, energy, and turbulence equations to address disturbances caused by mechanical agitation.

The research object is a 1,000 m³ floating roof storage tank with a simplified structure in which the bottom, side walls, and roof are boundaries. Three-dimensional models of the computational domain are used. The initial conditions for the simulation are a uniform temperature (T_0) and zero velocity at time t = 0. The experimental verification conditions included an initial temperature of 37.5 °C, an ambient temperature of 10 °C, a liquid level of 30 cm, and a stirring rate of 50 rpm using water. The simulation compared the effects of agitation on different observation methods. Validation was performed by comparing numerical simulation results with experimental results, showing a relative error of 15%. Mechanical stirring improves the uniformity of temperature distribution in jet heating, increasing the average oil velocity from 0.011 m/s to 0.098 m/s and the average temperature by 0.14°C. In tubular heating, however, mechanical agitation has a more significant effect: the average velocity increases 13.8-fold, and the average temperature rises 0.245 °C. The synergistic effect of tubular heating and oil reception increases the oil temperature by 21% compared to their separate use [46]. Under jet heating (Figure 9), mechanical stirring has little effect on the temperature distribution along the central line. The temperature profile and the increase over time remain similar with and without stirring in this central region. Under tubular heating (Figure 10), mechanical stirring has a significant effect, leading to a more uniform temperature distribution and an accelerated temperature rise along the central line compared to the non-stirred case. Efficiency was also found to increase by 8.37% on tubular heating. An increase in the nozzle outlet temperature

significantly changes the volumetric types of oil exiting the jet nozzle from the crude oil in the tank. The number of vortices increases proportionally with the flow rate of hot crude oil through the nozzle. Turbulence spreads rapidly across the entire tank surface in all directions, accelerating the heating and mixing of oil in the tank. However, the same nozzle outlet velocity at higher temperatures can reduce the operational mixing time of crude oil. The volume method is used for computational domain discretization. A refined grid is used in areas with intense heat transfer and flow. The computational domain is divided based on the oil heating rate into significant influence zones, indirect influence zones, and minimal influence zones, as shown in Figure 12 [35], [42].

Table 8. Subjects related to temperature control of storage tank.

No.	Scholars	Subjects	Findings
1	Sani et al. [44]	Improving crude oil storage tank heating and blending using multiple hot jet sprays.	Increasing the Froude Number can increase crude oil's heating and blending process. This can be done by increasing the nozzle outlet temperature, the temperature in the storage tank, or the nozzle flow rate.
2	Lei et al. [45]	Effect of mechanical stirring on heat transfer and flow of crude oil in storage tanks under different heating methods	The storage tank's velocity and temperature distribution pattern are better for jet heating than for tubular heating. However, mechanical stirring in tubular heating significantly impacts the most efficient energy consumption.
3	Sun et al. [43]	main influencing factors of waste heat utilization effectiveness in the tank storage receiving process of waxy crude oil under dynamic liquid level conditions	Liquid level dynamics, mixing conditions, and the external thermal environment influence waste heat utilization in the crude oil receiving process.
4	Sun et al. [40]	heat flow transfer characteristics and main influencing factors of waxy crude oil tank during storage heating process under dynamic thermal conditions	The circumferential effect of the heating coil increases the convective heat transfer in the tank. The closer the coil distribution is on both sides of the tank, the more significant the impact on heat transfer reduces the low-temperature zone at the bottom.
5	Zhao et al. [35]	Numerical simulation of tubular heating in waxy crude oil vault tank based on VOF model	A stable single vortex structure is formed in the gas region, while the water at the bottom of the tank maintains a stable double vortex.
6	Li et al. [42]	Numerical study on oil temperature field during extended storage in large floating roof tank	Double-deck floating roofs were found to have better thermal insulation capabilities than single-deck.
7	Zhao et al. [46]	Heat transfer characteristics of oil receiving and delivering process: Crude oil storage tanks	The combined effect of tubular heating and oil reception and delivery results in an average temperature increase of 21% higher than the sum of the two processes.
8	Dong et al. [41]	Heat transfer research on the cooling process of waxy crude oil storage in the vault tank based on the VOF model	The crude oil cooling mechanism in the dome-shaped storage tank can prevent operational problems due to temperature stratification and oil freezing

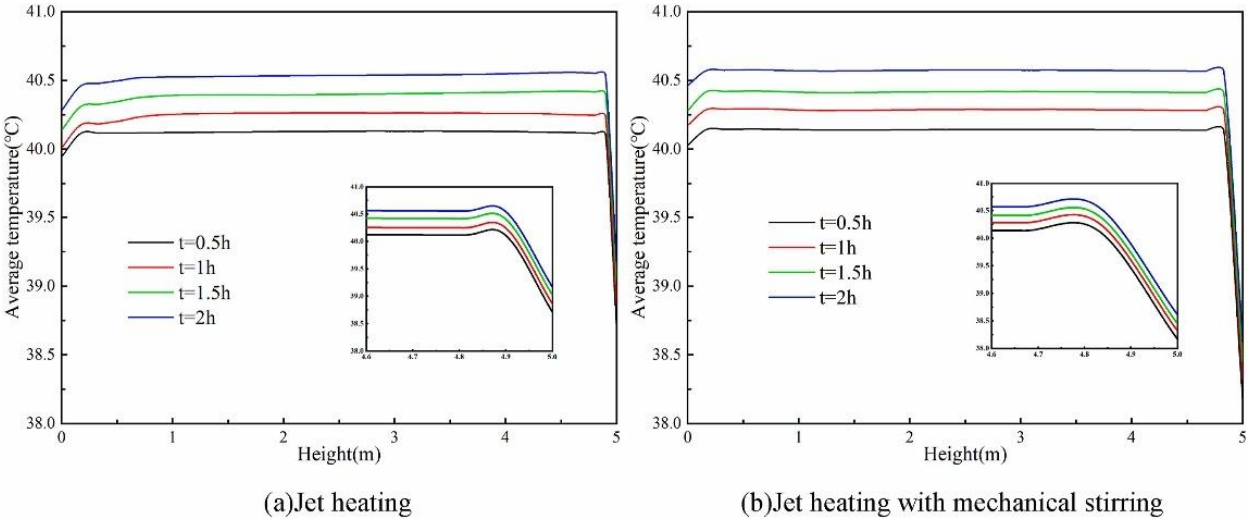

Figure 9. (a) Jet heating velocity field. (b) Jet heating with mechanical stirring [45].

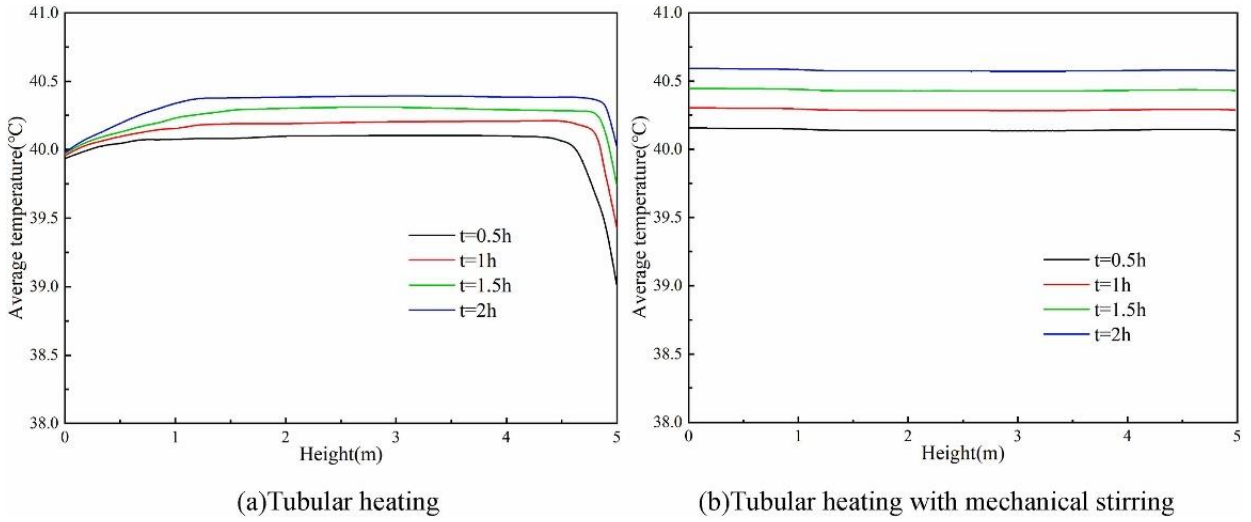

Figure 10. (a) Tubular heating velocity. (b) Tubular heating velocity with mechanical stirring [45].

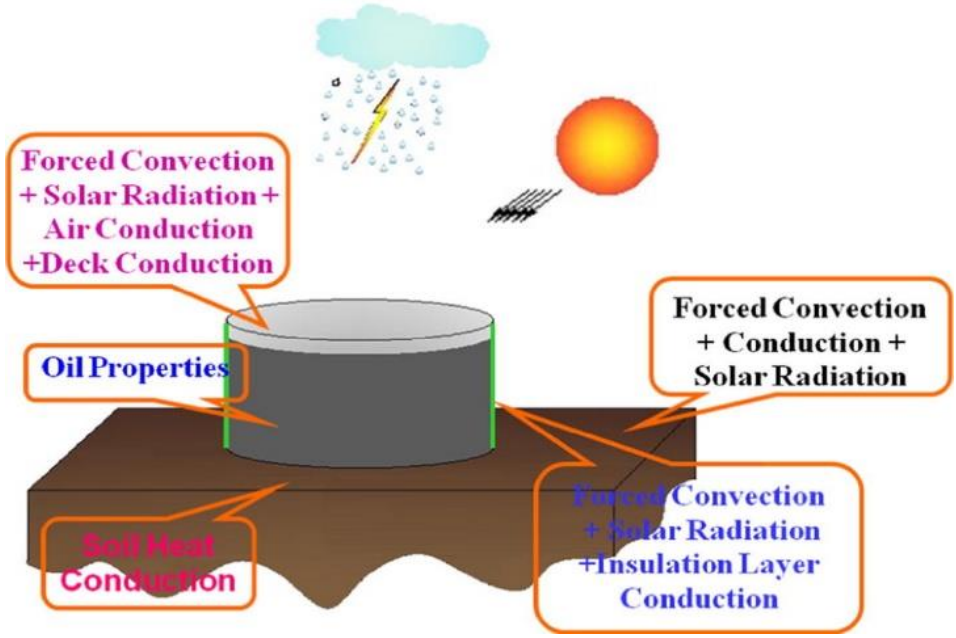

Figure 11. Scheme of heat transfer [42].

Processing, storage, and distribution of oil, incredibly waxy crude oil with a large density, easy-to-freeze properties, and high viscosity, has high rheological properties that require qualified technology in its implementation [46]. In practice, tank heating engineering has challenges of high energy consumption and carbon emissions [42]. When waxy crude oil is heated, there is a change from the gel state to the sol state and then to liquid. In the gel state to the sol state, the porous system formed by wax crystals is slowly destroyed, and the resistance to crude oil flow is reduced by increasing temperature. In the receiving process, the temperature difference between hot and cold oil forms an inhomogeneity in the density field. The influence of field inhomogeneity is that the heat flow diffusion stage has a faster duration, so the mixing speed and the effect of temperature are weaker. The ambient temperature is the main factor in heat dissipation. Optimal measures are required in the storage tank to maintain a favorable temperature or heating process [45]. Research [35] understands the characteristics of heat transfer and flow in the tank during tubular heating. The VOF model was used to capture the interfacial reactions of oil, gas, and water, and the porous media method was used to represent the structure of the oil gel. Physical and mathematical models are built to process the heating process of tubular crude oil in a dome tank, which is solved discretely by the finite volume method. The dimensions of the dome tank with a volume of 300 m^3 are used as the research object, with three heating tubes installed in the tank. There are three stages in the simulation: the first is thermal diffusion, the global thermal response stage, and the stable heating stage.

The experimental conditions for validation involved a scaled tank with a radius of 0.3875 meters and a center height of 0.8012 meters, with 8-millimeter-thick insulation wrapped around the side walls. Six temperature sensors were installed. The specific experimental conditions included an initial average crude oil temperature of 35 °C, an initial temperature difference between sensors of no more than 0.1 °C, a bottom liquid water level of 0.02 m, a waxy crude oil liquid level of 0.5 m, a tank top gas space, a constant heating tube working temperature of 80 °C, and an ambient temperature of 5 °C. At the thermal diffusion stage, the crude oil around the tube undergoes initial heating to form a thermal response zone. The gas at the top experiences rapid cooling at a rate of 8.54°C/ hour, while the water at the bottom of the tank experiences brief cooling for 35 minutes before starting to heat up at a rate of 0.44°C/hour. When convective heat transfer is substantial, the gas above the tank absorbs more heat from the crude oil, causing a slower cooling rate [41]. The interface phase is detected with VOF in conditions where gas, crude oil, and water coexist. The formed vortex continues to grow, affecting the oil-gas and oil-water interfaces. In the global thermal response stage, the vortex of the crude oil area continues to grow and reduces the temperature difference throughout the tank. The gas in the tank experiences stable heating at a rate of 0.37°C/hour. The final stage is stable heating; the heating distribution throughout the tank becomes uniform. Crude oil and water on the surface base experience heating at the same rate of 0.117°C/hour. Given the relatively short heating duration, natural convection and thermal conductivity are the main factors influencing the physical field [35].

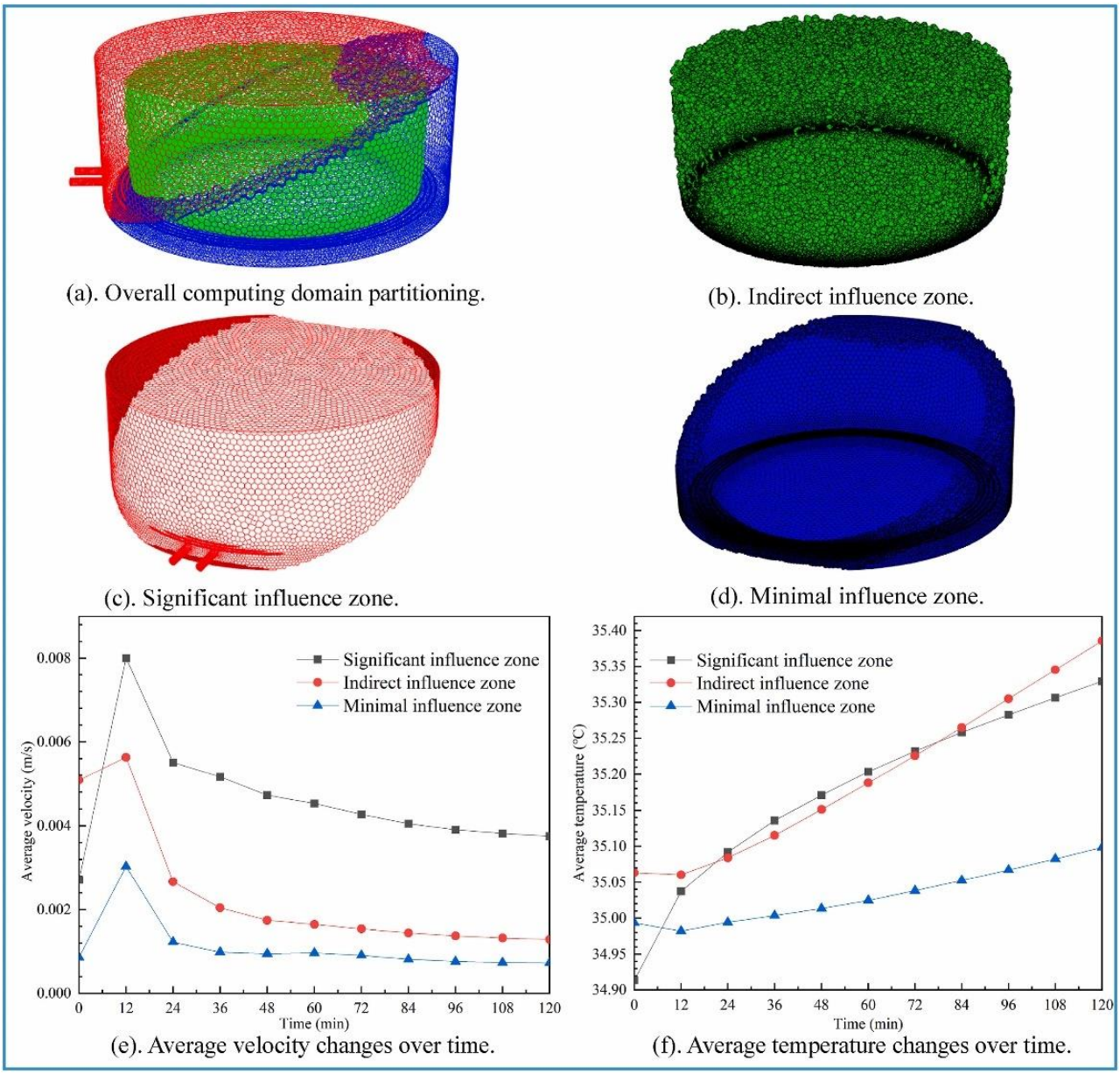

Figure 12. Display of the computational domain in different zones [46].

4.2 Failure and hazard of oil storage tank

Biodiesel in Indonesia is a mixture of 35%-v biodiesel and 65%-v petrodiesel. As a result, the risk of storage tank corrosion increases due to biological influences. Although biodiesel is more environmentally friendly, it has several weaknesses, namely high polarity, and is susceptible to oxidation due to its oxygen content. In a fuel storage tank system, there are four corrosion zones: the top of the tank, the splashing zone, the liquid zone, and the bottom. The bottom of the tank is the part most susceptible to microbiologically influenced corrosion because this part has the most direct contact with water, dissolved salts, organic and inorganic deposits [50]. Common failures in the oil and gas industry storage tanks include corrosion, cracking due to local settlement, and weld failure. Research [52] focuses on the case of bottom plate cracks caused by a combination of corrosion and local settlement. Visual inspection was taken as a sample for analysis, located near the cleaning door, with a length of 1000 mm and 1430 mm. The chemical composition of Q345R shows an excess of S, V, and Ti elements and a deficiency of Al, causing the material to be challenging but brittle. FEA was performed to study the cracks on the bottom plate of a crude oil storage tank. The simulation focused on the area near the cleanout door and used a model based on the tank's actual dimensions. The model included the reinforcing plates on the inner and outer sides of the cleanout door.

The analysis considered the effects of gravity and internal pressure from the stored crude oil. The results showed that stress was concentrated at the corner between the cleanout door and the bottom plate, primarily due to local settlement. Additionally, stress levels in this zone could exceed the material's yield strength when the tank is filled. Further SCC (stress corrosion cracking) testing confirmed that the tank's material (Q345R) is vulnerable to cracking in a hydrogen sulfide environment, which increases the risk of failure under these conditions.

Apart from oil and gas industry equipment, stored products also have their risks of danger, such as radiation, the spread of toxins, and environmental damage. Over 42% of fire accidents at refineries or fuel storage terminals are caused by “pool fires”. Leaks from storage tanks trigger fluids to flow out and are directly exposed to the environment, which can cause oil liquids to evaporate and spread. The risk of tank leaks can cause explosions, fires, and domino effects that worsen accidents. The risk of tank leaks can cause explosions, fires, and domino effects that worsen accidents. Factors such as the height and diameter of the leak hole play a role in determining the characteristics of the exit fluid flow, which can influence the level of danger posed. The height of the hole affects the rate of leakage flow; the higher the rate, the slower and the smaller the horizontal distance of the flow. Then, the hole diameter affects the flow velocity, but with the same discharge [28], [47]. Tank leaks can cause explosions, fires, and domino effects that can worsen accidents. Infrastructure components must be carefully designed to ensure safety and smooth operations. Explosions can be caused by "pool fires" or intentional detonations. Explosions can result in tank failures, leading to buckling or wrinkling of the tank shell. Investigating explosions is challenging and costly if done through experimentation. Therefore, computational methods are recommended because they do not require physical objects, thereby minimizing the risk of accidents. Research [49] focuses on the finite element analysis (FEA) method, in which blast loads are represented by an assumed time-dependent impulsive pressure that varies around the circumference based on empirical evidence. The pressure distribution was modeled exponentially in time and space. To illustrate how full-size tanks behave under sudden pressure from a nearby explosion, this study examined several tank sizes. The vertical cylindrical shell examined in this study has a fixed flat roof and clamped boundary conditions at the bottom. Assuming uniform thickness for simplicity, this shell has D = 15 m, H = 12 m, h = 7.5 mm, and H/D = 0.8 and R/h = 1000. The natural period of dynamic response is t_n = 135 ms. A commonly accepted range for considering an impulsive load is when the ratio to/tn becomes 0.22. Dynamic analysis was performed using Abaqus Dynamic Explicit software. Deformation magnitude is directly proportional to tank pressure; deformation progresses from plastic to buckling as pressure increases. Compared to tank height and diameter, shell thickness is the most significant factor influencing the buckling limit [49].

Table 9. Subjects related to failure and hazard in the storage tank.

No.	Scholars	Subjects	Findings
1	Qi et al. [47]	Quantitative risk assessment of crude oil storage tank leakage accident based on fuzzy Bayesian network and improved AHP.	The study shows that the proposed method can effectively identify LACOST probability and consequence changes, enabling decision-makers to optimize risk management strategies and achieve efficient resource allocation.
2	Heidarinejad et al. [48]	Investigating radiation, toxic, and hot gases fire hazards in large-scale storage tanks for oil derivatives with and without wind conditions	Increasing wind speed from zero to 15 m/s results in a 1.5-fold increase in safe distance. Without wind, CO and CO_2, as well as high-temperature gases, do not pose a damaging threat.
3	Godoy et al. [49]	Plastic buckling of oil storage tanks under blast loads	The main variables influencing the changes in shell properties are identified through the total plastic energy, which depends on the shell thickness and the minor influence of height and altitude.

4	Aslan et al. [50]	Microbiologically influenced corrosion in B35 carbon steel storage tank: The influence of diesel blend sludge mixed culture in the oil-water interphase	The occurrence of MIC in the oil-water interface by mixed cultures of diesel sludge can cause a uniform corrosion rate on carbon steel with a value of 0.05 mm/year (Medium category). Increasing the amount of biofuel acid beyond the permitted limits causes fuel degradation by the presence of microorganisms.
5	Zhou et al. [51]	Dynamic risk analysis of oil depot storage tank failure using a fuzzy Bayesian network model	The BT model mapped to FBN is considered more effective in assessing the probability of storage tank failure than fuzzy set theory and the multi-expert judgment method.
6	Zhang et al. [52]	Failure analysis of local settlement induced Q345R bottom plate cracking of crude oil storage tank	Q345R is susceptible to H_2S stress corrosion cracking according to the SCC test. Stress corrosion cracking (SCC) on the base plate occurs under working conditions containing H_2S and is influenced by uneven soil settlement in the storage tank.

After a fire, other dangers that arise are just as dangerous; radiation and the spread of pollutants become dangers with long-term damage, which influence and affect the surrounding environment. By evaluating using numerical, analytical, and experimental methods, it is hoped that the risk of these dangers can be prevented and their impact reduced. In the FDS software, with Large Eddy Simulation (LES), the fire simulation involves turbulence, non-premixed conditions, and diffusion behavior. In addition, the Large Eddy Simulation (LES) method can be used to study the vortex structure in oil flows, which will validate experimental data from crude oil storage tanks. The heterogeneity of the density field is helpful as an indicator of the effectiveness of waste heat utilization. The lower the heterogeneity, the better and more efficient the oil mixing [43]. The objective of the simulation is to review three fuels, gasoline, kerosene, and crude oil, that spread radiation to the environment. Environmental conditions are essential in reviewing radiation, especially wind factors, because, without wind, CO, CO_2, and high gas temperatures do not cause destructive hazards.

Research [48] considered real-scale tanks with diameters of 25, 50, and 75 m. The tank height was fixed at 15 m. The researchers scrutinized three standard refinery fuels: gasoline, kerosene, and crude oil. Scenarios included conditions with and without wind influence. Four wind modes were considered: zero speed and speeds ranging from 5 to 15 m/s. Other environmental factors were constant, such as pressure, temperature, humidity, and species mass fraction. The geometry involved a 4 m x 4 m square fire pool within a 12 m x 12 m x 12 m domain to validate the temperature. Boundary conditions were applied 4 m from the borders of the fuel bed. To validate radiation, experiments were conducted using tanks with diameters of 30 and 50 m containing a 20 cm layer of water and a 2 cm layer of kerosene on the surface. The study results are shown in Figure 14, which shows no significant risk in the absence of wind, radiation, and emissions, with a safe distance of about 2.8 times the tank diameter and a fixed height of 15 m. Wind speed affects the spread of hazards up to 5 meters from the ground surface at a wind speed of 15 m/s. The tank diameter only affects the radiation range in the interval of 47 to 117 meters when the tank diameter increases from 25 to 75 meters [48]. Wind speed affects almost 50% of the temperature drop, while the bottom temperature of the tank affects 40-60%. [53]According to the research paper's results [49], Wind speed affects the spread of hazards up to 5 meters from the ground surface at a wind speed of 15 m/s.

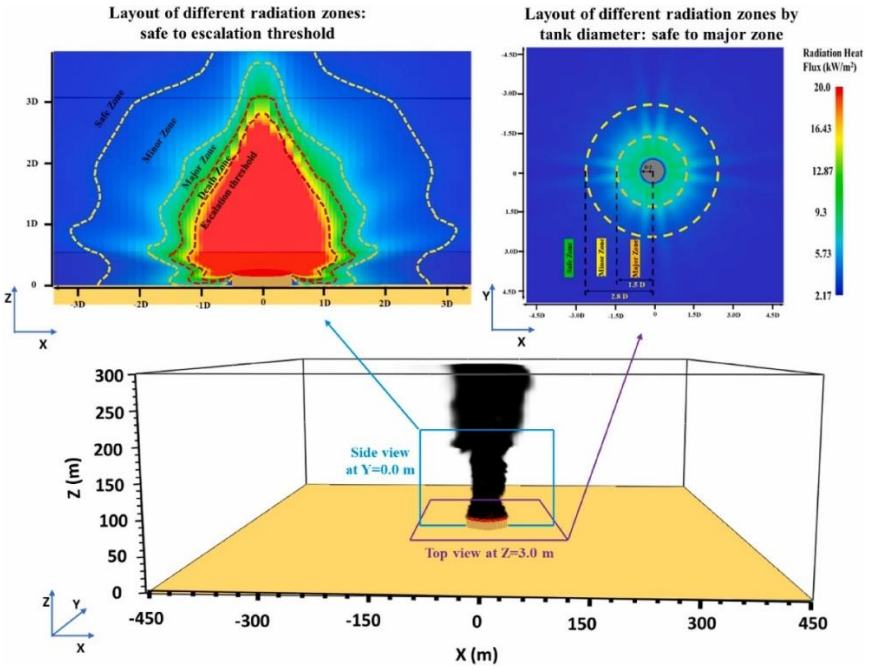

Figure 13. Layout of various radiation zones at Y = 0 (side view) and Z = 3.0 m (top view) generated by a gasoline tank fire with a 75-meter diameter, under no-wind conditions. [48].

The strength and durability of the storage tank are needed for the smooth distribution of oil. The materials stored at refineries or oil and gas terminals are flammable and poisonous. Infrastructure components must be designed carefully, for the safety and smooth running of work. The risk of fire and explosion is likely high in the oil and gas industry. Explosion accidents can be caused by "pool fire" or deliberate detonation. The explosion caused severe damage to oil storage tanks. Tank failure due to explosion can be in the form of buckling or wrinkles on the tank shell. Explosion investigation is complicated, requires high costs, and is dangerous if identified by experiment. Therefore, the computational method is recommended because it does not require real objects, so the risk of accidents can be minimized. Focusing on the FEA method, it examines several pressure and explosion scenarios to understand the elastic limit and the transition to buckling. The amount of deformation is directly proportional to the pressure value in the tank so that as the pressure increases, the deformation develops from plastic to buckling. Shell thickness is the most significant factor influencing the buckling limit rather than tank height and diameter [49].

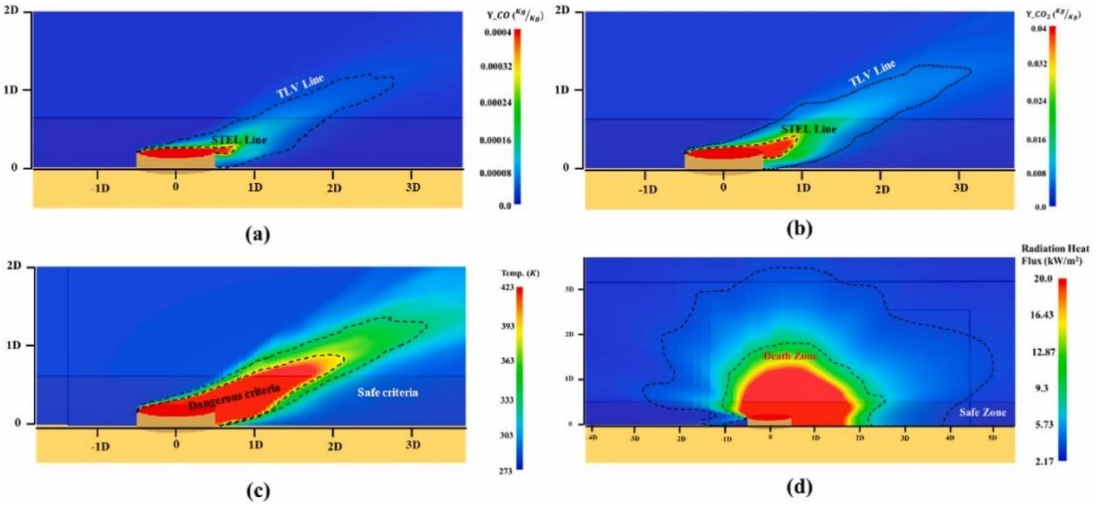

Figure 14. The emission contour of (a) CO, (b) CO_2 species, (c) temperature, and d) radiation for the condition of wind speed of 15 m/s and fuel tank of 75 m of gasoline in the middle plane Y = 0 [48].

5 Conclusion and remarks

This review discusses several aspects of the causes and effects of failures in several energy industry infrastructures, using several methods to improve productivity and safety. Based on a comprehensive study of infrastructure failures, it plays an essential role in the energy industry's safety, especially in oil and gas. Several vital notes are summarized as follows.

- Using new lubrication in MOVs can reduce thrust loss by 17.6% and improve performance under high differential pressure conditions.
- Using a probabilistic approach and a lognormal distribution for reliability analysis provides up to 5% higher damage prediction accuracy than traditional methods.
- High concentrations of NaCl, $CaCl_2$, S, and NAs in crude oil can cause corrosion, leading to failure and environmental problems. High temperatures or flow rates can also accelerate chemical reactions.
- Computational fluid dynamics (CFD) was used to model fluid flow in heavy crude oil pipelines with non-Newtonian models (Herschel–Bulkley and Bingham). The simulation results showed that the highest shear stress occurred on the outer wall of the elbow (extrados) due to an increase in flow velocity. This increase directly impacted local corrosion.
- CFD shows that heating the oil tank using tubular heating tubes and mechanical agitation increases the heat transfer efficiency by up to 21% compared to the single method. An increase in the liquid fraction volume of oil by 1.6% is also recorded in the 45° pipe inclination scenario. Using AI and RAM/FMEA/FMECA methods with the SSTIM (Shortening Surveillance Test Interval Method) can reduce unavailability by up to 82%, compared to testing with fixed intervals.
- A combination of tube heating and mechanical agitation increases the efficiency of oil tank heating by 21% compared to using a single system.
- Efficiency improvement of 8.37% with the tubular heating method when mechanical agitation is applied.
- A dynamic FEA simulation of a 15-meter-diameter, 12-meter-tall tank shows that the impulsive pressure caused by an explosion result in nonlinear deformation, increasing from plastic to buckling. The shell's thickness (7.5 mm) is the dominant factor in the buckling limit, surpassing the tank's height and diameter influence.

Several methods, such as RAM, PRA, FMEA, and FMECA, are methods or approaches for reliability analysis, maintenance, and system testing. Combining two or more methods can improve the efficiency and effectiveness of the process. Overall, this paper highlights the numerical approach method to be utilized in efforts to improve safety, reliability, and efficiency in the energy industry. Numerical methods are essential for maintaining performance and determining regular maintenance cycles. Meanwhile, FEA and CFD methods can help detect failures earlier so mitigation decisions are determined long before failure occurs. All methods contained in this paper allow design optimization, risk reduction, and cost reduction for experiments and make workers effective and safe.

References

1. A. M. Moghani and R. Loni, “Review on energy governance and demand security in oil-rich countries,” Jan. 01, 2025, *Elsevier Ltd*. doi: 10.1016/j.esr.2024.101625.
2. C. Difiglio, “Oil, economic growth and strategic petroleum stocks,” *Energy Strateg. Rev.*, vol. 5, pp. 48–58, Dec. 2014, doi: 10.1016/j.esr.2014.10.004.
3. T. Zhu, J. Balakrishnan, and G. J. C. da Silveira, “Bullwhip effect in the oil and gas supply chain: A multiple-case study,” *Int. J. Prod. Econ.*, vol. 224, Jun. 2020, doi: 10.1016/j.ijpe.2019.107548.
4. A. Okeke, “Towards sustainability in the global oil and gas industry: Identifying where the emphasis lies,” *Environ. Sustain. Indic.*, vol. 12, Dec. 2021, doi: 10.1016/j.indic.2021.100145.
5. L. Herlina *et al.*, “Indonesia’s country-specific CO2 emission factor based on gas fuels for greenhouse gas inventory in the energy sector,” *Environ. Pollut.*, vol. 368, Mar. 2025, doi: 10.1016/j.envpol.2025.125749.
6. I. Hardi, M. Afjal, M. Can, G. M. Idroes, T. R. Noviandy, and R. Idroes, “Shadow economy, energy consumption, and ecological footprint in Indonesia,” *Sustain. Futur.*, vol. 8, Dec. 2024, doi: 10.1016/j.sftr.2024.100343.

7. R. Gyambrah, M. An, and E. Stemn, “Practitioners’ perspectives on health and safety risk management in the Ghanaian oil and gas industry,” *Saf. Sci.*, vol. 177, Sep. 2024, doi: 10.1016/j.ssci.2024.106579.
8. N. Grabill, S. Wang, H. A. Olayinka, T. P. De Alwis, Y. F. Khalil, and J. Zou, “AI-augmented failure modes, effects, and criticality analysis (AI-FMECA) for industrial applications,” *Reliab. Eng. Syst. Saf.*, vol. 250, Oct. 2024, doi: 10.1016/j.ress.2024.110308.
9. Z. Yang, L. Xu, K. Zhang, and W. Zhu, “Numerical study on benefits of curved serrations upon suppressing turbulent boundary layer trailing-edge noise,” *Phys. Lett. Sect. A Gen. At. Solid State Phys.*, vol. 530, Jan. 2025, doi: 10.1016/j.physleta.2024.130131.
10. T. Takami, S. Matsui, M. Oka, and K. Iijima, “A numerical simulation method for predicting global and local hydroelastic response of a ship based on CFD and FEA coupling,” *Mar. Struct.*, vol. 59, pp. 368–386, May 2018, doi: 10.1016/j.marstruc.2018.02.009.
11. M. Suliman, M. Ibrahim, E. A. Algehyne, and V. Ali, “A study of an efficient numerical method for solving the generalized fractional reaction-diffusion model involving a distributed-order operator along with stability analysis,” *Comput. Math. with Appl.*, vol. 180, pp. 61–75, Feb. 2025, doi: 10.1016/j.camwa.2024.12.006.
12. R. W. Ahmad, K. Salah, R. Jayaraman, I. Yaqoob, and M. Omar, “Blockchain in oil and gas industry: Applications, challenges, and future trends,” *Technol. Soc.*, vol. 68, Feb. 2022, doi: 10.1016/j.techsoc.2022.101941.
13. I. Masudin, N. Tsamarah, D. P. Restuputri, T. Trireksani, and H. G. Djajadikerta, “The impact of safety climate on human-technology interaction and sustainable development: Evidence from Indonesian oil and gas industry,” *J. Clean. Prod.*, vol. 434, Jan. 2024, doi: 10.1016/j.jclepro.2023.140211.
14. I. Animah, “Real-time monitoring of life extension risk in the offshore oil & gas sector,” *J. Loss Prev. Process Ind.*, vol. 94, Apr. 2025, doi: 10.1016/j.jlp.2025.105566.
15. J. Kim, S. H. Lee, and S. K. Kim, “Transient analysis of lubrication with a squeeze film effect due to the loading rate at the interface of a motor operated valve assembly in nuclear power plants,” *Nucl. Eng. Technol.*, vol. 55, no. 8, pp. 2905–2918, Aug. 2023, doi: 10.1016/j.net.2023.02.008.
16. D. W. Kim, S. G. Park, S. C. Kang, and Y. S. Kim, “A study on the phenomenon of rate of loading in motor operated gate valves,” *Nucl. Eng. Des.*, vol. 240, no. 5, pp. 957–962, May 2010, doi: 10.1016/j.nucengdes.2010.01.013.
17. D. W. Kim, S. G. Park, S. C. Kang, S. G. Lee, and S. Y. Hong, “Analysis of the effect of lubrication performance on motor operated valve actuator output thrust,” *Nucl. Eng. Des.*, vol. 241, no. 8, pp. 2716–2721, Aug. 2011, doi: 10.1016/j.nucengdes.2011.06.007.
18. S. Kang, S. Park, D. Lee, Y. Kim, and D. Kim, “A study on the stem friction coefficient behavior of motor-operated valves,” in *Nuclear Engineering and Design*, Mar. 2011, pp. 961–967. doi: 10.1016/j.nucengdes.2011.01.017.
19. S. Parsaei, A. Pirouzmand, M. R. Nematollahi, A. Ahmadi, and M. R. Zerehpoosh, “Risk-effective optimal maintenance regime for a periodically tested safety component subjected to imperfect repair,” *Ann. Nucl. Energy*, vol. 211, Feb. 2025, doi: 10.1016/j.anucene.2024.110902.
20. S. Parsaei, A. Pirouzmand, M. R. Nematollahi, A. Ahmadi, and K. Hadad, “Effect of test-caused degradation on the unavailability of standby safety components,” *Nucl. Eng. Technol.*, vol. 56, no. 2, pp. 526–535, Feb. 2024, doi: 10.1016/j.net.2023.10.029.
21. I. Martón, P. Martorell, R. Mullor, A. I. Sánchez, and S. Martorell, “Optimization of test and maintenance of ageing components consisting of multiple items and addressing effectiveness,” Sep. 01, 2016, *Elsevier Ltd*. doi: 10.1016/j.ress.2016.04.015.
22. Y. C. Li *et al.*, “Risk evaluation for motor operated valves in an Inservice Testing Program at a PWR nuclear power plant in Taiwan,” *Int. J. Press. Vessel. Pip.*, vol. 90–91, pp. 17–21, Feb. 2012, doi: 10.1016/j.ijpvp.2011.10.003.
23. S. M. Shin, I. S. Jeon, and H. G. Kang, “Surveillance test and monitoring strategy for the availability improvement of standby equipment using age-dependent model,” *Reliab. Eng. Syst. Saf.*, vol. 135, pp. 100–106, 2015, doi: 10.1016/j.ress.2014.11.001.
24. K. Ting, Y. C. Li, K. T. Chen, F. T. Chien, G. D. Li, and S. H. Huang, “Risk-informed developments and comparisons for the safety related valves of Inservice Testing Program at Taiwan BWR and PWR nuclear power plants,” *Int. J. Press. Vessel. Pip.*, vol. 117–118, pp. 70–75, 2014, doi: 10.1016/j.ijpvp.2013.10.012.
25. G. S. Song and M. C. Kim, “Comparison of state-of-knowledge correlation effect associated with lognormal, beta, and gamma uncertainty distributions,” *Reliab. Eng. Syst. Saf.*, vol. 245, May 2024, doi: 10.1016/j.ress.2024.110033.

26. M. C. Kim, “Rigorous derivation of interfacing system LOCA frequency formulas for probabilistic safety assessment of nuclear power plants,” *Reliab. Eng. Syst. Saf.*, vol. 238, Oct. 2023, doi: 10.1016/j.ress.2023.109470.
27. S. Kordalivand, R. Akbari, and M. Abbasi, “Quantifying the impact of risk mitigation measures using SPAR-H and RCM Approaches: Case study based on VVER-1000 systems,” *Nucl. Eng. Des.*, vol. 423, Jul. 2024, doi: 10.1016/j.nucengdes.2024.113174.
28. Y. Ge *et al.*, “Numerical investigation on oil leakage and migration from the accidental hole of tank wall in oil terminal of pipeline transportation system,” *J. Pipeline Sci. Eng.*, vol. 4, no. 2, Jun. 2024, doi: 10.1016/j.jpse.2024.100175.
29. M. Meriem-Benziane, B. Bou-Saïd, B. G. Nasser Muthanna, and I. Boudissa, “Numerical study of elbow corrosion in the presence of sodium chloride, calcium chloride, naphthenic acids, and sulfur in crude oil,” *J. Pet. Sci. Eng.*, vol. 198, Mar. 2021, doi: 10.1016/j.petrol.2020.108124.
30. M. Hosseini, E. Ghalyani, and N. Ghorbani Amirabad, “Development of double-variable seismic fragility functions for oil refinery piping systems,” *J. Loss Prev. Process Ind.*, vol. 68, Nov. 2020, doi: 10.1016/j.jlp.2020.104259.
31. H. M. Tawancy, L. M. Al-Hadhrami, and F. K. Al-Yousef, “Analysis of corroded elbow section of carbon steel piping system of an oil-gas separator vessel,” *Case Stud. Eng. Fail. Anal.*, vol. 1, no. 1, pp. 6–14, Jan. 2013, doi: 10.1016/j.csefa.2012.11.001.
32. A. Coulon, R. Salanon, and L. Ancian, “Innovative numerical fatigue methodology for piping systems: Qualifying Acoustic Induced Vibration in the Oil&Gas industry,” in *Procedia Engineering*, Elsevier Ltd, 2018, pp. 762–775. doi: 10.1016/j.proeng.2018.02.072.
33. J. Hu, “Prediction of the internal corrosion rate for oil and gas pipelines and influence factor analysis with interpretable ensemble learning,” *Int. J. Press. Vessel. Pip.*, vol. 212, Dec. 2024, doi: 10.1016/j.ijpvp.2024.105329.
34. M. Meriem-Benziane, B. Bou-Saïd, and N. Boudouani, “The effect of crude oil in the pipeline corrosion by the naphthenic acid and the sulfur: A numerical approach,” *J. Pet. Sci. Eng.*, vol. 158, pp. 672–679, Sep. 2017, doi: 10.1016/j.petrol.2017.08.073.
35. J. Zhao, F. Li, C. Qu, C. Sun, and H. Dong, “Numerical simulation of tubular heating in waxy crude oil vault tank based on VOF model,” *Appl. Therm. Eng.*, vol. 262, Mar. 2025, doi: 10.1016/j.applthermaleng.2024.125083.
36. P. Chen and X. Liu, “Stress prediction of heated crude oil pipeline in permafrost region via fully coupled heat-moisture-stress numerical simulation and SVM algorithm,” *Tunn. Undergr. Sp. Technol.*, vol. 139, Sep. 2023, doi: 10.1016/j.tust.2023.105210.
37. R. K. Ratnakar, S. Pandian, H. Mary, and H. Choksi, “Flow assurance methods for transporting heavy and waxy crude oils via pipelines without chemical additive intervention,” 2024, *KeAi Publishing Communications Ltd.* doi: 10.1016/j.ptlrs.2024.07.005.
38. Y. Kanoun, A. M. Aghbash, T. Belem, B. Zouari, and H. Mrad, “Failure prediction in the refinery piping system using machine learning algorithms: classification and comparison,” in *Procedia Computer Science*, Elsevier B.V., 2024, pp. 1663–1672. doi: 10.1016/j.procs.2024.01.164.
39. L. Zhang, C. Du, H. Wang, and J. Zhao, “Three-dimensional numerical simulation of heat transfer and flow of waxy crude oil in inclined pipe,” *Case Stud. Therm. Eng.*, vol. 37, Sep. 2022, doi: 10.1016/j.csite.2022.102237.
40. W. Sun, Y. Liu, M. Li, Q. Cheng, and L. Zhao, “Study on heat flow transfer characteristics and main influencing factors of waxy crude oil tank during storage heating process under dynamic thermal conditions,” *Energy*, vol. 269, Apr. 2023, doi: 10.1016/j.energy.2023.127001.
41. H. Dong, S. Zhang, J. Zhao, Q. Cheng, and X. Liu, “Heat transfer research on the cooling process of waxy crude oil storage in the vault tank based on VOF model,” *Appl. Therm. Eng.*, vol. 258, Jan. 2025, doi: 10.1016/j.applthermaleng.2024.124657.
42. W. Li, Q. Shao, and J. Liang, “Numerical study on oil temperature field during long storage in large floating roof tank,” *Int. J. Heat Mass Transf.*, vol. 130, pp. 175–186, Mar. 2019, doi: 10.1016/j.ijheatmasstransfer.2018.10.024.
43. W. Sun, X. Zhang, B. Liu, L. Zhao, Q. Cheng, and Z. Wang, “Analysis of the main influencing factors of waste heat utilization effectiveness in the tank storage receiving process of waxy crude oil under dynamic liquid level conditions,” *Renew. Energy*, vol. 228, Jul. 2024, doi: 10.1016/j.renene.2024.120707.
44. M. S. Sani, D. D. Ganji, A. Ramiar, and K. Hoseinzadeh, “Improving crude oil storage tank heating and blending using multiple hot jet sprays: An experimental and numerical study,” *Case Stud. Therm. Eng.*, vol. 65, Jan. 2025, doi: 10.1016/j.csite.2024.105547.
45. M. Lei, J. Zhao, H. Wang, and X. Zhou, “Effect of mechanical stirring on heat transfer and flow of crude oil in

storage tanks under different heating methods," *Case Stud. Therm. Eng.*, vol. 58, Jun. 2024, doi: 10.1016/j.csite.2024.104382.
46. J. Zhao, M. Li, S. Liu, and H. Dong, "Heat transfer characteristics of oil receiving and delivering process in crude oil storage tanks," *Case Stud. Therm. Eng.*, vol. 61, Sep. 2024, doi: 10.1016/j.csite.2024.104994.
47. S. Qi, J. Shuai, L. Shi, Y. Li, and L. Zhou, "Quantitative risk assessment of leakage accident of crude oil storage tank based on fuzzy Bayesian network and improved AHP," *J. Loss Prev. Process Ind.*, vol. 90, Aug. 2024, doi: 10.1016/j.jlp.2024.105341.
48. G. Heidarinejad, M. Eftekhari, M. Safarzadeh, and M. Z. Targhi, "Investigating radiation, toxic and hot gases fire hazards in large-scale storage tanks for oil derivatives with and without wind conditions," *Int. J. Therm. Sci.*, vol. 208, Feb. 2025, doi: 10.1016/j.ijthermalsci.2024.109504.
49. L. A. Godoy and M. P. Ameijeiras, "Plastic buckling of oil storage tanks under blast loads," *Structures*, vol. 53, pp. 361–372, Jul. 2023, doi: 10.1016/j.istruc.2023.04.057.
50. C. Aslan *et al.*, "Microbiologically influenced corrosion in B35 carbon steel storage tank: The influence of diesel blend sludge mixed culture in the oil-water interphase," *Case Stud. Chem. Environ. Eng.*, vol. 10, Dec. 2024, doi: 10.1016/j.cscee.2024.101022.
51. Q. Y. Zhou, B. Li, Y. Lu, J. Chen, C. M. Shu, and M. shu Bi, "Dynamic risk analysis of oil depot storage tank failure using a fuzzy Bayesian network model," *Process Saf. Environ. Prot.*, vol. 173, pp. 800–811, May 2023, doi: 10.1016/j.psep.2023.03.072.
52. Z. Shuxin *et al.*, "Failure analysis of local settlement induced Q345R bottom plate cracking of crude oil storage tank," *Heliyon*, vol. 8, no. 11, Nov. 2022, doi: 10.1016/j.heliyon.2022.e11952.
53. W. Sun *et al.*, "Study of main factors influencing unsteady-state temperature drop in oil tank storage under dynamic thermal environment coupling," *Pet. Sci.*, vol. 20, no. 6, pp. 3783–3797, Dec. 2023, doi: 10.1016/j.petsci.2023.08.003.